

Characterization of hydroxycinnamic acid derivatives binding to bovine serum albumin†

Xiao-Ling Jin, Xia Wei, Feng-Ming Qi, Sha-Sha Yu, Bo Zhou* and Shi Bai*

Received 1st February 2012, Accepted 24th February 2012

DOI: 10.1039/c2ob25237f

Hydroxycinnamic acid derivatives (HCAs) are a group of naturally occurring polyphenolic compounds which possess various pharmacological activities. In this work, the interactions of bovine serum albumin (BSA) with six HCA derivatives, including chlorogenic acid (CHA), caffeic acid (CFA), *m*-coumaric acid (*m*-CA), *p*-coumaric acid (*p*-CA), ferulic acid (FA) and sinapic acid (SA) have been investigated by NMR spectroscopic techniques in combination with fluorescence and molecular modeling methods.

Competitive STD NMR experiments using warfarin sodium and L-tryptophan as site-selective probes indicated that HCAs bind to site I in the subdomain IIA of BSA. From the analysis of the STD NMR-derived binding epitopes and molecular docking models, it was deduced that CHA, CFA, *m*-CA and *p*-CA show similar binding modes and orientation, in which the phenyl ring is in close contact with protein surface, whereas carboxyl group points out of the protein. However, FA and SA showed slightly different binding modes, due to the steric hindrance of methoxy-substituents on the phenyl ring.

Relaxation experiments provided detailed information about the relationship between the affinity and structure of HCAs. The binding affinity was the strongest for CHA and ranked in the order CHA > CFA > *m*-CA ≥ *p*-CA > FA > SA, which agreed well with the results from fluorescence experiments. Based on our experimental results, we also conclude that HCAs bind to BSA mainly by hydrophobic interaction and hydrogen bonding. This study therefore provides valuable information for elucidating the mechanisms of BSA–HCAs interaction.

Introduction

The interactions between biological macromolecules and small molecules have attracted great interest in recent years.^{1–3} Among bio-macromolecules, serum albumin is the major soluble protein constituent of the circulatory system and has many physiological functions. It acts as a transport protein for many endogenous and exogenous compounds and plays a pharmacological role in the colloid blood pressure and maintenance of blood pH value.^{4–6} Therefore, studies on the binding of drugs with albumin can provide useful information of the metabolism and transporting process of drugs, and hence become an important research field in chemistry, life sciences and clinical medicine.^{7,8} In addition, drug–albumin complex may be considered as a model for gaining general fundamental insights into drug–protein binding, because of the availability, stability, and extraordinary binding capacity of albumin.⁹ In this regard, bovine serum albumin

(BSA) has been extensively studied because of its structural homology with human serum albumin (HSA).^{10–12}

Polyphenols, the biggest group of natural anti-oxidants, are widely distributed in the plant kingdom and are present in considerable amounts in fruits, vegetables, and beverages in the human diet.¹³ These compounds have attracted much attention due to their physiological functions, namely, in the prevention of coronary heart disease, cancer, and inflammation.^{14–16} Hydroxycinnamic acid derivatives (HCAs), such as chlorogenic, caffeic, *m*, *p*-coumaric, ferulic and sinapic acid, also known as phenolic compounds, comprise one of the largest and most ubiquitous groups of plant metabolites,¹⁷ and have been confirmed to possess multiple biological and pharmacological properties including antioxidant,^{18,19} antiviral,²⁰ antimicrobial,²¹ antityrosinase,²² hepatoprotective actions²³ and modulation of signal transduction pathway.²⁴ Interestingly, the difference of their structures leads to different effects in function. For example, Chiang *et al.*²⁵ showed that caffeic acid and chlorogenic acid which contain two hydroxyl groups in the phenyl ring exhibit more potent activity against herpesviruses and adenoviruses infections than those bearing one hydroxyl group such as ferulic acid and *p*-coumaric acid. Moreover, Wen *et al.*²⁶ determined the antimicrobial activity of several phenolic acids against five strains of *L. monocytogenes*, and found that cinnamic acid

State Key Laboratory of Applied Organic Chemistry, Lanzhou University, Lanzhou, Gansu 730000, China. E-mail: bozhou@lzu.edu.cn, bais@udel.edu; Fax: +86-931-8915557

† Electronic supplementary information (ESI) available: Fig. S1–S12 relating to STD-NMR spectra, the Stern–Volmer curves and double-log plots of fluorescence quenching of the HCAs. See DOI: 10.1039/c2ob25237f

exhibited the strongest activity, followed by *p*-coumaric, ferulic and caffeic acids, while chlorogenic acid was ineffective even at the maximum concentration tested (1.0% (w/v)). Their results suggested that increased hydroxylation of cinnamic acid molecule clearly reduced activity. These studies show that HCAs biological properties may depend both on their chemical structure, such as the number and position of the hydroxyl groups in the aromatic ring,^{27,28} and on their affinity with the molecules of enzymes and other biological macromolecules.^{29,30} Therefore, investigations on HCAs–BSA recognition processes may throw light on studies about drug metabolism and drug–protein interaction. In fact, there have been several studies on the interaction between various phenolic acids and BSA by means of fluorescence method.^{31,32} However, so far none of these investigations determined the binding epitope and evaluated binding modes and structure affinity in detail, which may limit our proper and comprehensive understanding of the interaction between HCAs and BSA.

NMR spectroscopy offers a variety of approaches for the characterization of drug–protein interactions,^{33–36} such as the saturation transfer difference (STD) NMR experiments for the analysis of binding epitopes at atomic resolution and the relaxation rate experiments for the investigation of binding affinity.^{37–40} In addition, fluorescence spectroscopy is also an appropriate method to study the interaction between drugs and proteins.^{41,42}

In the present work, we have employed a combination of NMR, fluorescence and computational techniques, in an attempt to determine where and how HCAs bind to BSA in solution. Several structural analogues of HCAs were investigated to identify the binding epitopes and their binding sites on BSA by STD NMR. ¹H NMR relaxation and fluorescence experiments ranked the analogues according to their relative binding affinity yielding detailed structure–affinity relations. Molecular docking was utilized to validate experimental data and to more accurately characterize the models of BSA–HCAs complexes. Our work thus is intended to provide a framework for elucidating the mechanisms of BSA–HCAs binding.

Experimental

Materials

Hydroxycinnamic acids derivatives, warfarin sodium (WAR) and L-tryptophan (L-Trp) and bovine serum albumin (molecular mass 66 200 Da) were purchased from Sigma Chemical Company and used without any further purification. D₂O and DMSO-*d*₆ at 99.9% purity was from Aldrich. All other reagents were of analytical grade.

NMR spectroscopy

All NMR data were obtained on Bruker Avance 400 MHz spectrometers at 298 K. Bruker software (topspin 2.1) was used to acquire and process NMR data.

In STD experiments, selective saturation of the protein was achieved by a train of Gaussian shaped pulses of 50 ms each, truncated at 1% and separated by a 1 ms delay. The duration of the presaturation of 3 s was adjusted using $n = 58$ cycles. Protein

resonance was suppressed by application of a 30 ms spin-lock pulse prior to acquisition. All STD experiments were selectively saturated using the Gaussian train pulses at -0.5 ppm for the on-resonance and 30 ppm for the STD control. The subtraction was performed after every scan, through a phase cycling. Samples contained 60 μ M protein and a ligand concentration of 10 mM HCAs respectively. In competitive STD experiments, samples were prepared with additional components as follows: 50 μ M BSA, 3 mM HCAs and 4.8 mM WAR/Trp. Intensities of all STD effects were calculated by division through integrals over the respective signals in ¹H NMR reference spectra. For group epitope mapping, these effects were then normalized against the largest STD effect observed, thus, 100% corresponds to the signal with the largest STD effect.

Spin–lattice relaxation rates were measured using the $(t-180^\circ-\tau-90^\circ)_n$ sequence. The τ values used for the selective and nonselective experiments were: 0.001, 0.005, 0.01, 0.02, 0.04, 0.06, 0.08, 0.12, 0.2, 0.4, 0.6, 1.0, 1.6, 2.4, 3.5, 5.0, 7.0, 10.0, 13.0, 18.0 s, respectively. The relaxation delay time t was set to be 15 s. The 180° selective inversion of proton spin population was obtained by a selective soft Gaussian perturbation pulse (width: 60 ms, power: 57.50 dB). The selective spin–lattice relaxation rates were calculated using the initial slope approximation and subsequent three-parameter exponential regression analysis of the longitudinal recovery curves. The maximum experimental error in the relaxation rate measurements was estimated to be 5%. The solutions for the relaxation rates experiments were obtained by dissolving the appropriate amounts of ligand and protein in DMSO-*d*₆–D₂O (8 : 92). In all experiments the ligand concentration was 10 mM and the protein concentration was 0, 15, 30, 45, 60, 75 μ M. The affinity index was calculated according to a method proposed by Martini *et al.*³⁹

Fluorescence spectroscopy

Fluorometric experiments were carried out on a LS-55 fluorescence spectrometer from Perkin Elmer. Stock solutions of HCAs (1 mM) in methanol and BSA (4 μ M) in 20 mM PBS (pH 7.4) were prepared at room temperature. The above solutions were stored in a refrigerator and used soon after. An appropriate quantity of HCAs solution was transferred to a 10.0 mL flask, and then 2.5 mL of BSA solution was added and diluted to 10.0 mL with PBS buffer. The final concentrations of HCAs were from 0.2 to 30.0 μ M with a constant BSA content of 1 μ M. The fluorescence spectra were recorded at $\lambda_{\text{exc}} = 280$ nm and λ_{em} from 300 to 500 nm. The intensity at 340 nm (tryptophan) was used to calculate the binding constant (K_a) based on the methods described previously.^{42,43}

Molecular docking

Molecular docking was carried out using software Autodock 4.2 and the Lamarckian genetic algorithm as a searching procedure.^{44,45} The structures of the ligand molecule were optimized using sybyl 6.9 and the PDB file of BSA was provided by Chi *et al.*⁴⁶ The grid maps were constructed using $60 \times 60 \times 60$ points, with a grid box point spacing of 0.375 Å and the grid center was set to 36, 5 and 7 Å. The AutoDocking parameters

used were, GA population size: 100; maximum number of energy evaluations: 2 500 000. Other parameters were set as default.⁴⁵ The resulting docking solutions were subsequently clustered with a root-mean-square deviation (rmsd) tolerance of 2.0 Å.

Results and discussion

STD NMR spectra

(i) Binding epitope mappings of HCAs to BSA. The STD NMR is a powerful method that can be used to detect ligand binding, as well as to determine ligand binding epitopes at an atomic resolution. We conducted the STD experiments using the six HCAs and BSA to gain insight into their interaction. The STD effects were observed for all the compounds, suggesting that all six HCAs are binding to BSA under our experimental conditions. As an example, Fig. 1 shows a STD spectrum of CHA in presence of BSA (for STD spectra of other compounds, please see the ESI†). The relative STD effects have been calculated as described in Experimental section. These values reflect the relative amount of saturation transferred from the protein onto the ligand. Protons with a high STD value are assumed to be in more intimate contact with the protein surface than those with lower STD values. The binding epitopes of HCAs are summarized in Fig. 2.

CHA, CFA, *m*-CA and *p*-CA show an almost identical binding epitope. Strong STD effects between 80–100% were observed for the phenyl protons, revealing the aromatic group is in close proximity to the protein surface. In addition, decrease in STD intensities, ranging from 89% to 61%, for double bond protons were observed in the direction toward the carboxyl group, indicating that the double bond is also involved in binding. Thus it can be deduced that the four compounds bind to BSA in a similar binding pattern, in which the phenyl group of HCAs is in close contact with BSA binding pocket, while hydrophilic groups (carboxyl groups) is oriented away from the binding pocket towards the solvent.

Comparatively, the epitopes determined for FA and SA show some differences. It was found, for FA, an introduction of a methoxy group at C-3 in the aromatic ring, significantly decreased STD intensities of H-2 of phenyl ring. Moreover, to SA, introducing two methoxy groups at C-3 and C-5 led to a decrease in STD intensities of the remaining phenyl proton, whereas H-7 shows a strongest STD effect. The STD data presented here indicate, when the methoxyl groups substitute for phenyl protons, steric hindrance of methoxyl may result in less pronounced binding of phenyl ring with the protein, while the moiety of double bond makes closer contacts with the protein in the binding pocket.

Interestingly, for CHA, the signal for quinate was nearly not detectable in the STD NMR spectrum (Fig. 1), indicating that this unit makes weaker contacts with the protein surface and may be more exposed to the solvent. This observation is consistent with the conclusions by Xiao *et al.* who proposed that the glycosyl, in general, does not play a significant role in the binding of ligand to BSA.⁴¹

(ii) Identification of the binding sites on BSA. BSA is a heart-shaped protein composed of three homologous mains (I–III). Each domain contains two subdomains named A and B. The principal regions of ligand binding sites of albumin are located in hydrophobic cavities in subdomains IIA and IIIA. To identify the binding sites of HCAs to BSA, competition STD experiments were performed using WAR⁴⁷ and Trp⁴⁸ as specific displacement marker ligands for site I (subdomains IIA) and site II (subdomains IIIA), respectively (see Fig. 3 and Fig. S6–S10†). The results reported in Table 1 showed that the STD amplification factors⁴⁹ of CFA, *m/p*-CA, FA and SA on BSA decreased after addition of WAR while the addition of Trp did not significantly change the STD amplification factors value. This indicates that WAR can displace HCAs but Trp has no effect on binding of the compounds to BSA. Overall, the competition experiments

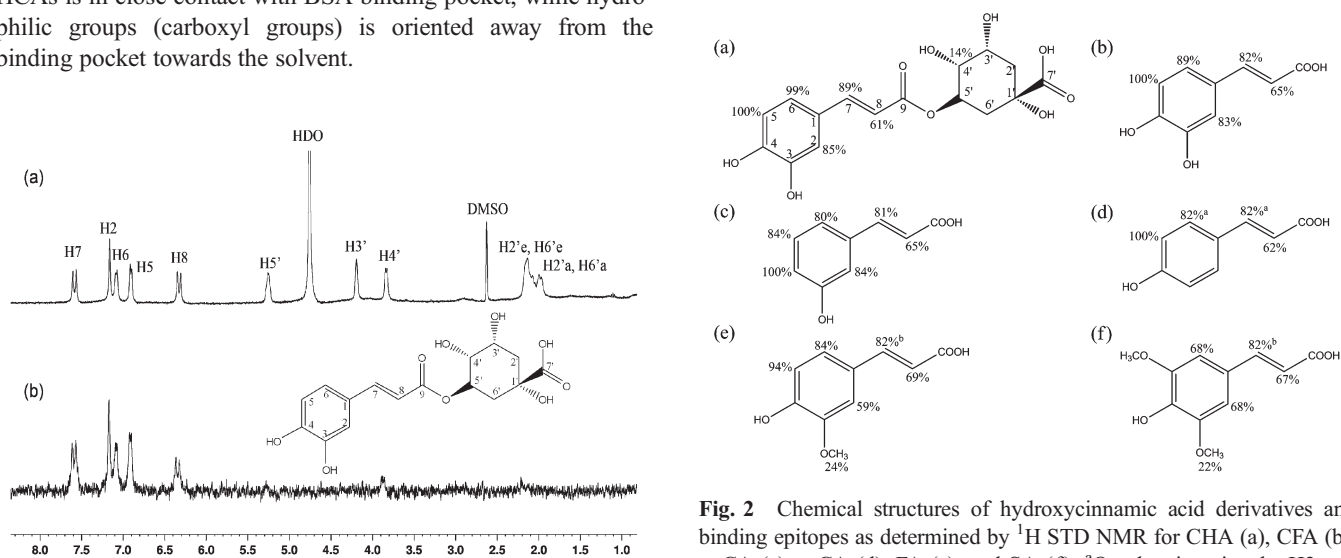


Fig. 1 ¹H NMR spectrum (a) and ¹H STD NMR spectrum (b) of CHA in the presence of BSA. Spectra taken at 298 K on a 400 MHz spectrometer with a room temperature probe. NS = 256, TD = 32 K, sat pulse = −0.5 ppm for 3.0 s (see Methods).

Fig. 2 Chemical structures of hydroxycinnamic acid derivatives and binding epitopes as determined by ¹H STD NMR for CHA (a), CFA (b), *m*-CA (c), *p*-CA (d), FA (e), and SA (f). ^aOverlapping signals: H2 and H7 of *p*-CA. ^bTo simplify the direct comparison of the epitopes, the STD values for the H-7 of FA and SA were set to 82%, referring to that of H-7 of *p*-CA, and all the others for the remaining protons were normalized to this value.⁵⁷

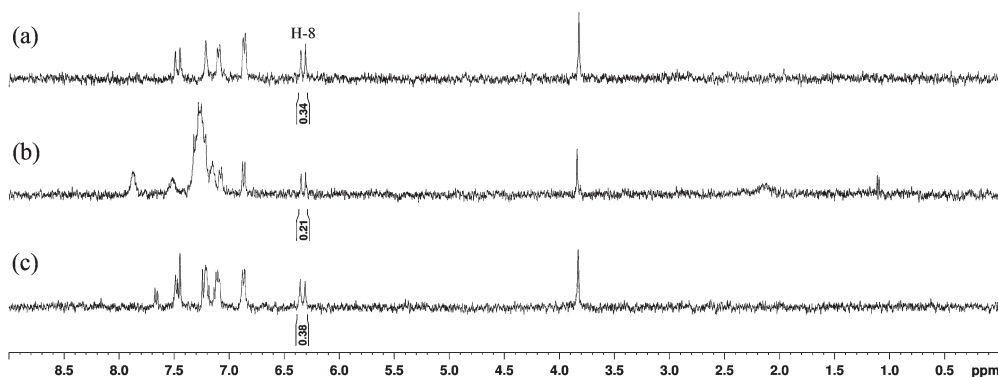


Fig. 3 (a) ^1H STD NMR of 50 μM BSA, 3 mM FA without the site probe; (b) ^1H STD NMR of 50 μM BSA, 3 mM FA in the presence of 4.8 mM WAR; (c) ^1H STD NMR of 50 μM BSA, 3 mM FA in the presence of 4.8 mM Trp. The STD effects of H-8, calculated as I_{STD}/I_0 , were shown in the figure. Spectra were taken at 298 K on a 400 MHz spectrometer with a room temperature probe. NS = 256, TD = 32 K, sat pulse = -0.5 ppm for 3.0 s (see Methods).

Table 1 STD amplification factors (A_{STD}^a) for H-8 of 3 mM HCAs in the presence of 50 μM BSA upon addition of 4.8 mM WAR or Trp

	CHA	CFA	<i>p</i> -CA	<i>m</i> -CA	FA	SA
A_{STD} (without the site probe)	46.2	24.0	25.2	30.6	20.4	10.2
A_{STD} (with WAR)	17.4	8.4	17.4	11.4	12.6	5.4
A_{STD} (with Trp)	21.6	24.6	27.0	28.8	22.8	9.6

^a STD amplification factors were calculated as $(I_{\text{STD}}/I_0) \times \text{ligand excess}$.⁴⁹

imply that the five HCAs interact with BSA at site I in sub-domain IIA. For the STD amplification factors of CHA, great changes were observed after addition of WAR, also a slight difference occurred while the addition of Trp. The data suggest that two binding sites are involved in the BSA–CHA interaction, and the predominant binding site for CHA is still located on site I (sub-domain IIA) of BSA, which is consistent with the earlier report.⁵⁰

Proton spin–lattice relaxation rates

It has been shown that selective spin–lattice relaxation rate R_1^{SE} values are sensitive probes of binding while non-selective R_1^{NS} values are not the case.⁵¹ Based on the comparison of selective (R_1^{SE}) proton spin–lattice relaxation rate of the ligand in the presence and absence of the macromolecular receptor, Rossi *et al.* have proposed the ‘affinity index’ as a measure of ligand–macromolecular affinity.⁵²

Assuming a fast chemical exchange between the free and bound environments, the experimentally observed selective relaxation rate $R_{1\text{obs}}^{\text{SE}}$ can be expressed by the following equation:

$$R_{1\text{obs}}^{\text{SE}} = x_f R_{1f}^{\text{SE}} + x_b R_{1b}^{\text{SE}} \quad (1)$$

where R_{1f}^{SE} and R_{1b}^{SE} are the selective spin–lattice relaxation rates for the free and bound ligands, respectively. Whereas χ_f

and χ_b are corresponding ligand fractions. If the ligand–receptor equilibrium was considered as follows:



With a thermodynamic equilibrium constant $K = [\text{ML}]/[\text{M}][\text{L}]$, assuming $[\text{L}] \gg [\text{M}_0]$, the difference in the spin–lattice relaxation rate, ΔR_1^{SE} , can be expressed as:

$$\Delta R_1^{\text{SE}} = \frac{KR_{1b}^{\text{SE}}}{1 + K[\text{L}]} [\text{M}_0] \quad (3)$$

where $\Delta R_1^{\text{SE}} = R_{1\text{obs}}^{\text{SE}} - R_{1f}^{\text{SE}}$ and $[\text{M}_0]$ is the initial concentration of macromolecule. Therefore, a plot of ΔR_1^{SE} versus $[\text{M}_0]$ will be a straight line passing through the origin and with a slope

$$[A]_L^T = \frac{KR_{1b}^{\text{SE}}}{1 + K[\text{L}]} \quad (4)$$

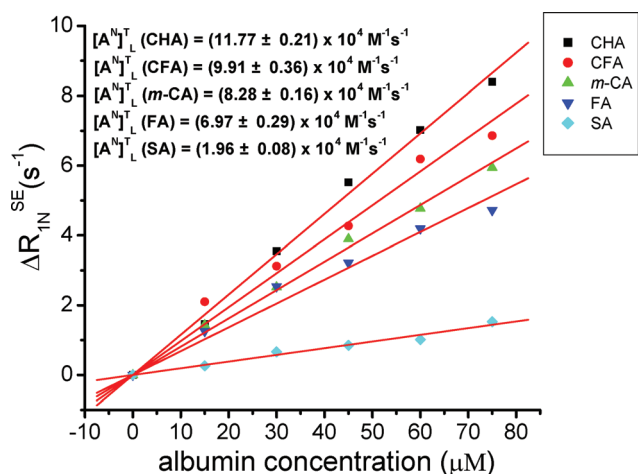
which is defined as the ‘affinity index’. The dimensions of $[A]_L^T$ are $\text{M}^{-1} \text{s}^{-1}$ and the superscript T and subscript L signify the temperature and ligand concentration at which the measurement was made. In order to eliminate the impacts of motional anisotropies and different spin densities at ligand proton sites, $[A]_L^T$ is then normalized to the relaxation rate of the free ligand and the ‘normalized affinity index’ $[A^N]_L^T$ is calculated. Therefore, $[A^N]_L^T$ is a more appropriate parameter to compare the recognition processes between a protein and different ligands.⁵²

^1H NMR spectra of the six HCAs were carefully analyzed and the signal H-7 was well resolved except for that of *p*-CA. Therefore, only the other five compounds were used for relaxation rate study because overlapping peaks are not appropriate for 180° shape pulse to get right selective R_1 . Table 2 shows the values of R_1^{SE} and R_1^{NS} of the H-7 proton of the studied HCAs in relation to albumin concentration.

The results show that for all HCAs studied here, in the absence of BSA, $R_1^{\text{NS}} > R_1^{\text{SE}}$, while with increasing protein concentration, R_1^{SE} becomes greater than R_1^{NS} . The increase in the selective relaxation rate implies a large contribution from the bound ligand fraction to the observed relaxation rate. This observation clearly suggests the presence of an interaction between the studied ligands and BSA. In order to evaluate the strength of

Table 2 Calculated R_1^{SE} and R_1^{NS} for the H-7 proton of HCAs as a function of albumin concentrations at 298 K

BSA concentration (μM)	CHA		CFA		<i>m</i> -CA		FA		SA	
	R_1^{SE} (s^{-1})	R_1^{NS} (s^{-1})	R_1^{SE} (s^{-1})	R_1^{NS} (s^{-1})	R_1^{SE} (s^{-1})	R_1^{NS} (s^{-1})	R_1^{SE} (s^{-1})	R_1^{NS} (s^{-1})	R_1^{SE} (s^{-1})	R_1^{NS} (s^{-1})
0	0.552	0.668	0.350	0.468	0.397	0.522	0.432	0.523	0.631	0.700
15	1.359	0.764	1.086	0.692	0.967	0.612	0.975	0.633	0.796	0.749
30	2.513	0.960	1.443	0.723	1.399	0.677	1.530	0.706	1.050	0.777
45	3.597	1.054	1.845	0.742	1.944	0.715	1.822	0.697	1.168	0.777
60	4.425	1.030	2.516	0.818	2.294	0.738	2.243	0.716	1.273	0.794
75	5.181	1.330	2.751	0.903	2.759	0.767	2.469	0.742	1.594	0.840

**Fig. 4** Linear regression analysis of H-7 selective relaxation enhancements, ΔR_{1N}^{SE} as a function of albumin concentration. The measurements refer to a 10 mM solution of HCAs at 298 K. The value of the normalized affinity indexes $[A^N]_L^T$ is also reported with the corresponding error.

the binding process, the 'normalized affinity indexes' $[A^N]_L^T$ for ligand–protein systems were obtained by linear regression analysis of ΔR_{1N}^{SE} versus albumin concentration (shown in Fig. 4). The normalized affinity indexes ($[A^N]_L^T$) obtained here indicate that the binding affinities of HCAs are ranked in the order of CHA > CFA > *m*-CA > FA > SA, which are in a good agreement with other studies.^{31,32}

It was found CHA and CFA with two phenolic hydroxy groups were tightly bound by the BSA than *m*-CA in which only one hydroxy group exists. It was also revealed that the affinity of CFA to BSA decreased with single substitution of methoxyl group in the aromatic ring. The affinity was further decreased when two methoxyl are substituted on the benzene ring. These results suggest the hydrogen bonding may take place between phenolic hydroxyl and the polar groups of BSA binding cavity. Once methoxyl substituted for phenyl proton, steric hindrance may take place, which may weaken the hydrogen bonding between the ligand and BSA.

Moreover, it was revealed that BSA showed a higher affinity to CHA [affinity index = $(11.77 \pm 0.21) \times 10^4 \text{ M}^{-1} \text{ s}^{-1}$] than that to CFA [affinity index = $(9.91 \pm 0.36) \times 10^4 \text{ M}^{-1} \text{ s}^{-1}$], which means the esterification of carboxyl group with quinic acid increases the affinity for BSA greatly. Thus we deduce that the presence of quinic acid group which consists of three hydroxyl

groups and a COOH group, for enhancing hydrogen bonding and electrostatic interaction with the bulk solvent, seems to increase the binding affinity of CHA to BSA.

The analysis of STD NMR data and relaxation rate analysis of HCAs show that the phenyl ring and phenolic hydroxyl of HCAs are the key functionalities for binding. The phenolic hydroxyl participates in hydrogen bonding with polar groups of BSA binding cavity, whereas the phenyl ring donates hydrophobic interaction with hydrophobic residues of the protein. It is clear the subtle difference in structure of the studied HCAs plays a key role in affecting binding processes with the protein.

Fluorescence spectroscopy

Fluorescence experiments were carried out taking advantage of the intrinsic tryptophan fluorescence of BSA to probe the interaction with HCAs derivatives. Fig. 5 shows the fluorescence spectra (at $\lambda_{\text{ex}} = 280 \text{ nm}$) obtained for BSA at pH 7.4 with these six HCAs as quenchers. It was found that fluorescence intensity of BSA gradually decreased with the increasing concentration of the six ligands. Furthermore, small red shifts of maximum λ_{em} (2–10 nm) were observed for all tested compounds, suggesting an increase in the polarity of the tryptophan environment.

For the fluorescence quenching measurement, the decrease in intensity is usually described by the well-known Stern–Volmer equation.⁵⁴ In the linear range of the Stern–Volmer regression curve (Fig. S11†), the average quenching constants (K_{SV}) and quenching rate constant (k_q) were determined and are listed in Table 3. All the values of k_q is 1000-fold higher than the maximum value possible for diffusion-limited quenching in water ($\sim 10^{10} \text{ M}^{-1} \text{ s}^{-1}$), which confirm that there is a specific interaction occurring between BSA and the HCAs studied here. Furthermore, the binding constant value (K_a) and the number of binding sites (n) can be obtained from the double-logarithm curve⁵⁵ (see Fig. S12†). Table 3 gives the corresponding calculated results. The values of binding constant (K_a) suggest BSA has moderate affinity to HCAs, because the documented K_a values⁴ of noncovalent association of BSA with drugs mostly rang from 10^4 – 10^6 M^{-1} . It is clear from Table 3 that the binding affinity is ranked in the order CHA > CFA > *m*-CA \geq *p*-CA > FA > SA. This order is consistent with that from the NMR analysis of relaxation rates where it is demonstrated that CHA forms a more stable complex with BSA than other compounds. Thus the significance of hydrophobic interaction and hydrogen bonding in the process of protein–ligand binding is further demonstrated through our fluorescence quenching measurements.

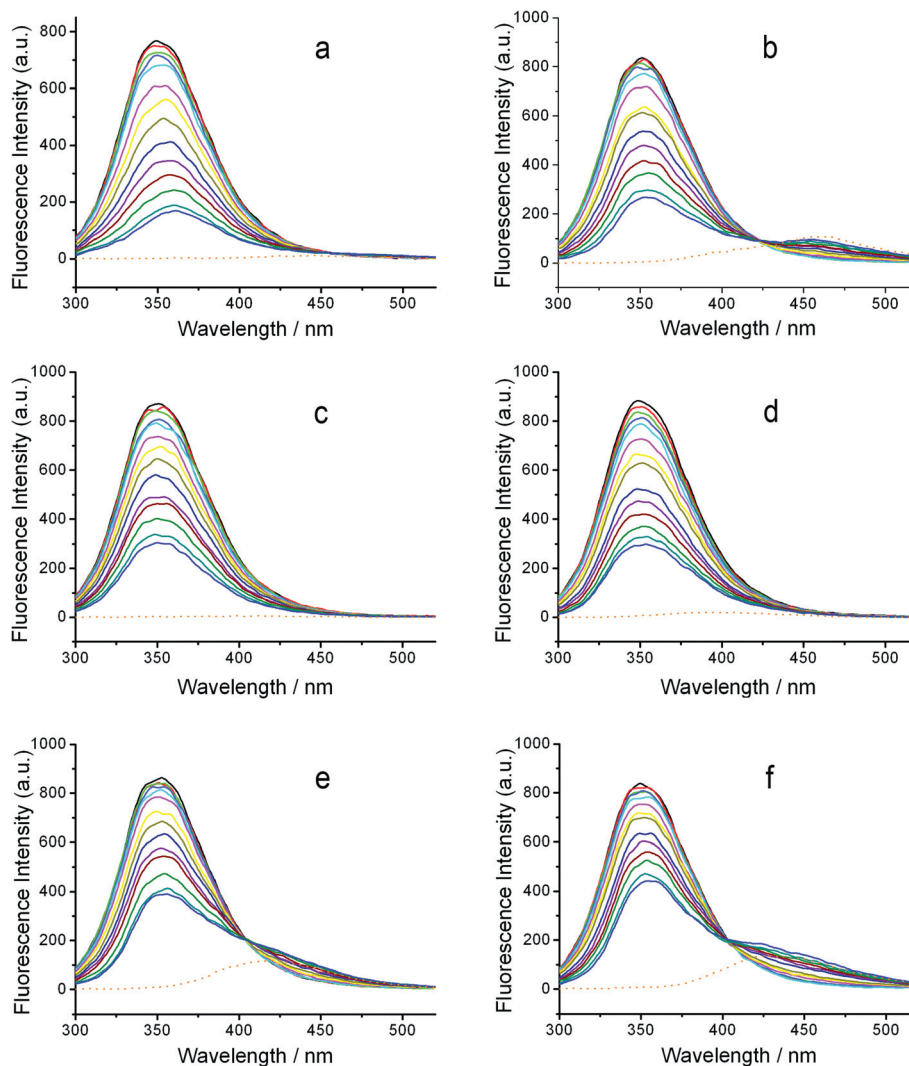


Fig. 5 Fluorescence quenching of BSA by CHA (a), CFA (b), *m*-CA (c), *p*-CA (d), FA (e), SA (f). From the top to the bottom the values of $C_{\text{drug}}/C_{\text{BSA}}$, were 0, 0.2, 0.4, 0.7, 1, 3, 5, 7, 10, 13, 16, 20, 25, 30, respectively; $\lambda_{\text{ex}} = 280 \text{ nm}$; $C_{\text{BSA}} = 1 \mu\text{M}$, $T = 298 \text{ K}$; the dotted line is the fluorescence spectrum of a native $30 \mu\text{M}$ ligand.

Table 3 Experimentally determined quenching and binding parameters for BSA–HCA complexes at 298 K

Compounds	$K_{\text{SV}} (10^4 \text{ M}^{-1})$	$k_{\text{q}} (10^{13} \text{ M}^{-1} \text{ s}^{-1})^a$	$K_{\text{a}} (\text{M}^{-1})$	n
CHA	9.03 ± 0.30	1.81 ± 0.06	$9.20 \times 10^4 \pm 1.56$	0.99 ± 0.04
CFA	5.57 ± 0.13	1.11 ± 0.03	$6.07 \times 10^4 \pm 1.40$	1.00 ± 0.03
<i>m</i> -CA	6.07 ± 0.14	1.21 ± 0.03	$1.14 \times 10^4 \pm 1.48$	0.86 ± 0.03
<i>p</i> -CA	6.67 ± 0.09	1.33 ± 0.02	$1.08 \times 10^4 \pm 1.34$	0.84 ± 0.02
FA	3.92 ± 0.12	0.73 ± 0.02	$0.51 \times 10^4 \pm 1.59$	0.82 ± 0.04
SA	3.00 ± 0.04	0.60 ± 0.01	$0.17 \times 10^4 \pm 1.45$	0.74 ± 0.03

^a The quenching rate constant (k_{q}) for all the HCAs were calculated using the equation $k_{\text{q}} = K_{\text{SV}}/\tau_0$, τ_0 is taken as $5 \times 10^{-9} \text{ s}$.⁵³

Molecular docking study

Molecular docking was performed to provide better understanding of the binding mode between HCAs and BSA. BSA and HSA have a homology similarity of 88% in their amino acid sequence.⁵⁶ The crystal structure of HSA is made up of three domains with similar structure in asymmetric and divided into

subdomains “A” and “B”. The binding site called site I in subdomain IIA is known to be a warfarin binding site or Sudlow’s site I, whereas site II is in subdomain IIIA and is known to be the very binding site of ibuprofen or Sudlow’s site II. The BSA model obtained shows the similarity in these two binding sites, and the binding sites for HCAs analyzed in this work have an equivalent binding site in HSA. Docking calculations were then

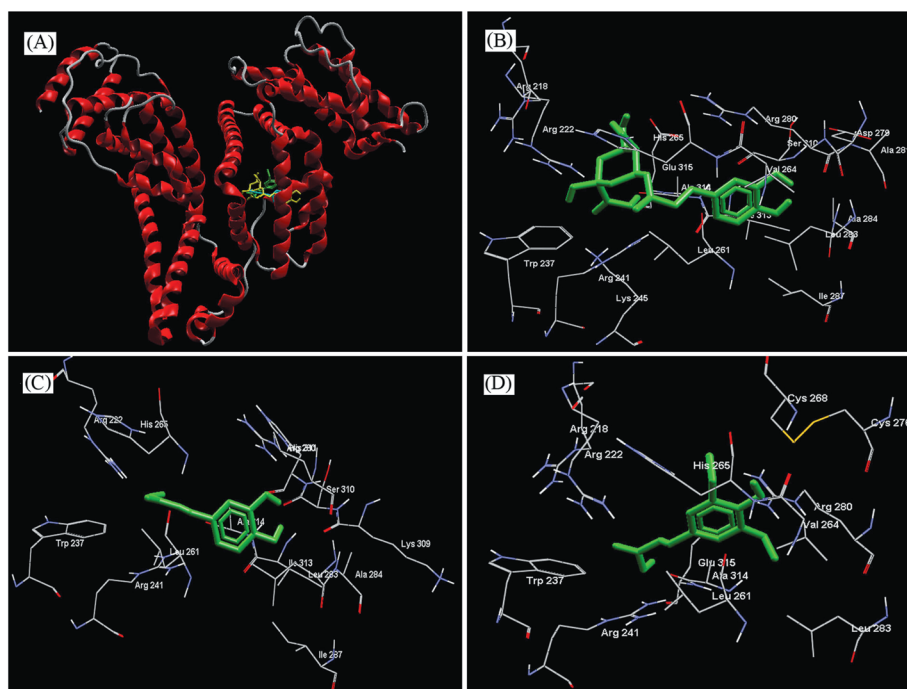


Fig. 6 Docking results of HCAs and BSA systems. (A) Overview of BSA structure and comparison of the binding models for the ligands used in this work. The ligands are shown in stick representation and colored as follows: CHA, yellow; CFA, blue; SA, green. (B), (C), (D) Conformation of CHA, CFA and SA in the binding site of BSA, respectively.

performed for HCAs with BSA binding site IIA, and the structures were selected according to the lowest binding free energy and considering they keep conformity with the STD NMR results. The docking results are shown in Fig. 6. Indeed, the binding mode obtained by docking was completely in agreement with that from the STD NMR data, thus validating the orientation of the six HCAs within the binding site. That is, CHA, CFA, *m*-CA and *p*-CA show similar binding mode and orientation, which the phenyl group is highly buried within the subdomain IIA hydrophobic cavity, whereas carboxyl group points out of the protein (Fig. 6B and 6C). In the case of FA and SA, the phenyl group has less intimate contact with the protein surface, due to the steric hindrance of methoxy-substituents on the phenyl ring (Fig. 6D). So we conclude that the binding of HCAs with BSA is mainly hydrophobic, mainly through the interaction between phenyl group and the main hydrophobic amino-acids of the site, such as Leu261, Leu283, Ile287, Ile313 and Ala314. There are also a number of specific hydrogen bonds between the phenolic hydroxyl (OH) groups of HCAs and polar residues nearby. For instance, CFA and CHA form two hydrogen bonds with the O atom of Ser310 and nitrogen atom of Arg280 side chains, respectively. The formation of hydrogen bonds thus stabilizes the HCA–BSA complex and participates in increasing the affinity of the binding region. In addition, the electrostatic force between hydrophilic carboxyl group of HCAs and amino group of Arg222 sidechain at the entrance of the cavity is also involved in the BSA–HCAs complex. This interaction is probably responsible for the location of double bond protons, which only make less critical hydrophobic contacts to the hydrocarbon chain of Arg241 and Leu261, consistent with less intense STD signals. Therefore, the results of molecular docking correlate

very well with the experimental NMR and fluorescence data and confirm that the interaction of HCAs with BSA are driven mainly by hydrophobic interaction and hydrogen bonding.

Conclusions

In this work, the interaction between the six HCAs and BSA has been investigated by NMR, fluorescence and computational techniques. The STD NMR data, assisted by docking calculations, reveal compounds CHA, CFA, *m*-CA and *p*-CA bind to BSA in a similar pattern, in which the phenyl group is in close contact with BSA binding pocket, while carboxyl group is oriented away towards the solvent. In contrast, FA and SA show somewhat different binding modes, due to the steric hindrance of methoxy-substituents on the phenyl ring. In addition, relaxation rate and fluorescence analysis provided quantitative information on the degree of affinity and structure of HCAs. The binding affinity of CHA and CFA, both having two phenolic hydroxyl groups, was higher than that of *m*-CA/*p*-CA with only one hydroxyl group. The affinity of SA to protein was found much smaller because of the steric hindrance of methoxy groups on the aromatic ring. The esterification of carboxyl group of CFA with quinic acid significantly increased the binding ability of CHA, probably due to solvation of quinic acid. We also conclude HCAs bind to BSA mainly by hydrophobic interaction and hydrogen bonding. Moreover, the results presented here demonstrate that the NMR method, especially when combined with other experimental means, provides a valuable tool for understanding interactions between BSA and ligands.

Acknowledgements

We thank Prof. R. T. Liu and his team at Shang Dong University for providing the PDB file for BSA. The work was supported by the Fundamental Research Funds for the Central Universities (Izujbky-2010-113), the 111 Project, and the National Natural Science Foundation of China (Grant No. 20972063).

References

- H. J. Bohm and G. Klebe, *Angew. Chem., Int. Ed. Engl.*, 1996, **35**, 2588–2614.
- L. Liang, H. A. Tajmir-Riahi and M. Subirade, *Biomacromolecules*, 2008, **9**, 50–56.
- S. Zheng, G. Kaur, H. Wang, M. Li, M. Macnaughtan, X. Yang, S. Reid, J. Prestegard, B. Wang and H. Ke, *J. Med. Chem.*, 2008, **51**, 7673–7688.
- D. C. Carter and J. X. Ho, *Adv. Protein Chem.*, 1994, **45**, 153–203.
- D. Shcharbin, M. Janicka, M. Wasiaak, B. Palecz, M. Przybyszewska, M. Zaborski and M. Bryszewska, *Biochim. Biophys. Acta*, 2007, **1774**, 946–951.
- D. Shcharbin, B. Klajnert, V. Mazhul and M. Bryszewska, *J. Fluoresc.*, 2005, **15**, 21–28.
- J. C. D'Eon, A. J. Simpson, R. Kumar, A. J. Baer and S. A. Mabury, *Environ. Toxicol. Chem.*, 2010, **29**, 1678–1688.
- N. Shahabadi, M. Maghsudi, Z. Kiani and M. Pourfoulad, *Food Chem.*, 2011, **124**, 1063–1068.
- D. P. Zhong, A. Douhal and A. H. Zewail, *Proc. Natl. Acad. Sci. U. S. A.*, 2000, **97**, 14056–14061.
- S. Dubeau, P. Bourassa, T. J. Thomas and H. A. Tajmir-Riahi, *Biomacromolecules*, 2010, **11**, 1507–1515.
- Z. X. Chi, R. T. Liu, Y. Teng, X. Y. Fang and C. Z. Gao, *J. Agric. Food Chem.*, 2010, **58**, 10262–10269.
- F. F. Tian, F. L. Jiang, X. L. Han, C. Xiang, Y. S. Ge, J. H. Li, Y. Zhang, R. Li, X. L. Ding and Y. Liu, *J. Phys. Chem. B*, 2010, **114**, 14842–14853.
- G. G. Duthie, S. J. Duthie and J. A. M. Kyle, *Nutr. Res. Rev.*, 2000, **13**, 79–106.
- A. Scalbert, C. Manach, C. Morand, C. Rémésy and L. Jiménez, *Crit. Rev. Food Sci. Nutr.*, 2005, **45**, 287–306.
- H. M. Rawel, J. Kroll and S. Rohn, *Food Chem.*, 2001, **72**, 59–71.
- C. Manach, A. Scalbert, C. Morand, C. Rémésy and L. Jiménez, *Am. J. Clin. Nutr.*, 2004, **79**, 727–747.
- C. A. Rice-Evans, N. J. Miller and G. Paganga, *Free Radical Biol. Med.*, 1996, **20**, 933–956.
- J. C. Cheng, F. Dai, B. Zhou, L. Yang and Z. L. Liu, *Food Chem.*, 2007, **104**, 132–139.
- X. L. Jin, R. T. Yang, Y. J. Shang, F. Dai, Y. P. Qian, L. X. Cheng, B. Zhou and Z. L. Liu, *Chin. Sci. Bull.*, 2010, **55**, 2885–2890.
- H. Tamura, T. Akioka, K. Ueno, T. Chujyo, K. Okazaki, P. J. King and W. E. Robinson Jr., *Mol. Nutr. Food Res.*, 2006, **50**, 396–400.
- J. P. Rauha, S. Remes, M. Heinonen, A. Hopia, M. Kähkönen, T. Kujala, K. Pihlaja, H. Vuorela and P. Vuorela, *Int. J. Food Microbiol.*, 2000, **56**, 3–12.
- H. S. Lee, *J. Agric. Food Chem.*, 2002, **50**, 1400–1403.
- V. Pérez-Alvarez, R. A. Bobadilla and P. Muriel, *J. Appl. Toxicol.*, 2001, **21**, 527–531.
- M. Nardini, F. Leonardi, C. Scaccini and F. Virgili, *Free Radical Biol. Med.*, 2001, **30**, 722–733.
- L. C. Chiang, W. Chiang, M. Y. Chang, L. T. Ng and C. C. Lin, *Antiviral Res.*, 2002, **55**, 53–62.
- A. Wen, P. Delaquis, K. Stanich and P. Toivonen, *Food Microbiol.*, 2003, **20**, 305–311.
- S. Adisakwattana, P. Moonsan and S. Yibchok-Anun, *J. Agric. Food Chem.*, 2008, **56**, 7838–7844.
- I. Medina, J. M. Gallardo, M. J. Gonzalez, S. Lois and N. Hedges, *J. Agric. Food Chem.*, 2007, **55**, 3889–3895.
- G. Bora-Tatar, D. Dayangaç-Erden, A. S. Demir, S. Dalkara, K. Yelekçi and H. Erdem-Yurter, *Bioorg. Med. Chem.*, 2009, **17**, 5219–5228.
- Y. Shi, Q. X. Chen, Q. Wang, K. K. Song and L. Qiu, *Food Chem.*, 2005, **92**, 707–712.
- S. Li, K. Huang, M. Zhong, J. Guo, W. Wang and R. Zhu, *Spectrochim. Acta, Part A*, 2010, **77**, 680–686.
- J. Kang, Y. Liu, M. X. Xie, S. Li, M. Jiang and Y. Wang, *Biochim. Biophys. Acta*, 2004, **1674**, 205–214.
- L. Fielding, *Curr. Top. Med. Chem.*, 2003, **3**, 39–53.
- C. Ludwig and U. L. Guenther, *Front. Biosci.*, 2009, **14**, 4565–4574.
- B. Becattini, C. Culmsee, M. Leone, D. Zhai, X. Zhang, K. J. Crowell, M. F. Rega, S. Landshamer, J. C. Reed, N. Plessnila and M. Pellicchia, *Proc. Natl. Acad. Sci. U. S. A.*, 2006, **103**, 12602–12606.
- B. A. Becker and C. K. Larive, *J. Phys. Chem. B*, 2008, **112**, 13581–13587.
- M. Mayer and B. Meyer, *Angew. Chem., Int. Ed.*, 1999, **38**, 1784–1788.
- P. M. Enriquez-Navas, M. Marradi, D. Padro, J. Angulo and S. Penadés, *Chem.–Eur. J.*, 2011, **17**, 1547–1560.
- S. Martini, M. Consumi, C. Bonechi, C. Rossi and A. Magnani, *Biomacromolecules*, 2007, **8**, 2689–2696.
- J. D. Figueroa-Villar and L. W. Tinoco, *Curr. Top. Med. Chem.*, 2009, **9**, 811–823.
- J. B. Xiao, H. Cao, Y. F. Wang, J. Y. Zhao and X. L. Wei, *J. Agric. Food Chem.*, 2009, **57**, 6642–6648.
- H. Liu, W. Bao, H. Ding, J. Jang and G. Zou, *J. Phys. Chem. B*, 2010, **114**, 12938–12947.
- Z. X. Chi and R. T. Liu, *Biomacromolecules*, 2011, **12**, 203–209.
- G. M. Morris, D. S. Goodsell, R. S. Halliday, R. Huey, W. E. Hart, R. K. Belew and A. J. Olson, *J. Comput. Chem.*, 1998, **19**, 1639–1662.
- R. Huey, G. M. Morris, A. J. Olson and D. S. Goodsell, *J. Comput. Chem.*, 2007, **28**, 1145–1152.
- Z. X. Chi, R. T. Liu, Y. Teng, X. Y. Fang and C. Z. Gao, *J. Agric. Food Chem.*, 2010, **58**, 10262–10269.
- G. Sudlow, D. J. Birkett and D. N. Wade, *Mol. Pharmacol.*, 1975, **11**, 824–832.
- K. J. Feske, W. E. Müller and U. Wollert, *Biochim. Biophys. Acta*, 1979, **577**, 346–359.
- M. Mayer and B. Meyer, *J. Am. Chem. Soc.*, 2001, **123**, 6108–6117.
- Y. J. Hu, C. H. Chen, S. Zhou, A. M. Bai and Y. Ou-Yang, *Mol. Biol. Rep.*, 2012, **39**, 2781–2788.
- G. Valensin, T. Kushnir and G. Navon, *J. Magn. Reson.*, 1982, **46**, 23–29.
- C. Rossi, C. Bonechi, S. Martini, M. Ricci, G. Corbini, P. Corti and A. Donati, *Magn. Reson. Chem.*, 2001, **39**, 457–462.
- A. Papadopoulou, R. J. Green and R. A. Frazier, *J. Agric. Food Chem.*, 2005, **53**, 158–163.
- J. R. Lakowicz, *Principles of Fluorescence Spectroscopy*, Springer, New York, 3rd edn, 2006.
- B. Sudhamalla, M. Gokara, N. Ahalawat, D. G. Amooru and R. Subramanyam, *J. Phys. Chem. B*, 2010, **114**, 9054–9062.
- S. N. Khan, B. Islam, R. Yennamalli, A. Sultan, N. Subbarao and A. U. Khan, *Eur. J. Pharm. Sci.*, 2008, **35**, 371–382.
- A. Blume, M. Berger, A. J. Benic, T. Peters and S. Hinderlich, *Biochemistry*, 2008, **47**, 13138–13146.